ISSN 1995-0780, Nanotechnologies in Russia, 2013, Vol. 8, Nos. 9–10, pp. 631–638. © Pleiades Publishing, Ltd., 2013.
Original Russian Text © A.P. Chumakov, I.V. Roslyakov, K.S. Napol'skii, A.A. Eliseev, A.V. Lukashin, H. Eckerlebe, W.G. Bouwman, D.V. Belov, A.I. Okorokov, S.V. Grigoriev, 2013, published in Rossiiskie Nanotekhnologii, 2013, Vol. 8, Nos. 9–10.

Influence of Substrate Microstructure on Longitudinal Correlation Length of Porous System of Anodic Alumina: Small-Angle Scattering Study

A. P. Chumakov[a], I. V. Roslyakov[b], K. S. Napol'skii[b], A. A. Eliseev[b], A. V. Lukashin[b], H. Eckerlebe[c], W. G. Bouwman[d], D. V. Belov[e], A. I. Okorokov[a], and S. V. Grigoriev[a]

[a] *Petersburg Nuclear Physics Institute, National Research Centre "Kurchatov Institute", Orlova roshcha, Gatchina, St. Petersburg, 188300 Russia*
[b] *Lomonosov Moscow State University, Moscow, 119991 Russia*
[c] *Helmholtz-Zentrum Geesthacht, Centre for Materials and Coastal Research, PO Box 1160 D- 21494, Geesthacht, Germany,*
[d] *Delft University of Technology, 2629 JB, Delft, The Netherlands*
[e] *Debye Institute for Nanomaterials Science, University of Utrecht, 3584 CH, Utrecht, The Netherlands*
e-mail: a.p.chumakov@gmail.com

Received December 25, 2012; accepted for publication June 6, 2013

Abstract—Three series of anodic alumina membranes have been studied using the small-angle diffraction of neutrons and synchrotron radiation. The samples are obtained by the oxidation of aluminum wafers by sulfuric and oxalic acids at various anodization voltages and differences in the distance between the pores. Using experiments on small-angle diffraction, a linear dependence between the average grain size of an initial aluminum wafer and the average rectilinearity of pores of the synthesized membranes is established. We suggest that the observed correlation is caused by the influence of the crystallographic orientation of grains of an initial aluminum wafer on the growth of a porous oxide film.

DOI: 10.1134/S106193481305002X

INTRODUCTION

The investigation into the processes of self-organization of nanostructures is a topical problem of modern material engineering. The membranes of anodic alumina (AA) are typical representatives of nanodimensional self-organized structures whose feature is a hexagonally ordered system of cylindrical pores, which is obtained as a result of the anodization of an aluminum substrate [1]. A change in the conditions of synthesis (composition of the electrolyte, applied voltage, quality of aluminum to be used, etc.) makes it possible to vary the diameter of pores, the degree of their ordering, and the thickness of the membrane in wide limits, making this method promising from the point of view of the development of porous structures of various functional applications [2–6]. It should be noted that the use of optimal parameters of synthesis makes it possible to achieve membranes with an extremely high degree of rectilinearity of pores and a hexagonal type of ordering of the channels close to an ideal one.

Porous AA films find applications in various spheres of science and engineering. They are used as inorganic membranes [7–9], a basis for the synthesis of nanocomposites or wirelike nanostructures [10–14], and two-dimensional photon crystals [15]. Examples of the creation of high-technological devices such as gas sensors, supercondensors, memory cells, etc. [1, 16–18], based on AA films are known. The quality of membranes and, hence, the materials based on them substantially affects their functional properties. In connection with the above, the development of efficient techniques for the fabrication of AA with an ordered porous structure and studying basic principles of its formation in combination with the development of the approval of spatially ordered nanomaterials are topical problems of the modern material engineering.

This work is a continuation of studies which we carried out earlier on the structure of AA membranes and its connection with the synthesis conditions. The use of small-angle techniques of neutron scattering (small-angle neutron scattering (SANS)) and of the synchrotron radiation (small-angle X-ray scattering (SAXS)) makes it possible to obtain data about the degree of the ordering of pores (longitudinal correlation length, average size of domains, and mozaic structure) in the whole sample volume [14–16]. We note that the often applied techniques of probe or electron microscopy give local information only about the surface of a porous film.

Structural parameters of films of anodic aluminum oxide according to the data of scanning electron microscope (SEM), small-angle scattering of neutrons (SANS), and SAXS

Names of samples	Conditions of acquisition (electrolyte, voltage, temperature)	Average size of crystallites of metal, mm^2	Thickness of membrane L, (according to SEM data), μm	Average distance between pores, nm			Diameter of pores (according to data SEM*), nm
				SEM*	SANS	SAXS	
AAS1	0.3 M H_2SO_4, 25 V, 2°C	0.427	10	63 ± 9	65.6	64.8	16 ± 1
AAS2		0.904	22		67.9	64.7	
AAS3		0.217	28		64.5	62.9	
AAS4		0.484	52		65.5	63.1	
AAO1	0.3 M $(COOH)_2$, 40 V, 2°C	0.381	10	102 ± 6	104.4	102.7	52 ± 3
AAO2		0.390	16		104.7	102.7	
AAO3		0.117	34		105.1	102.2	
AAO4		2.276	40		–	102.2	
HA1	0.3 M $(COOH)_2$, 140 V, −2°C	0.273	15	256 ± 27	220	222.1	193 ± 18
HA2		0.594	17	265 ± 25	239	299.5	
HA3		0.655	22	287 ± 19	283	304.8	
HA4		0.490	39	288 ± 24	288	290.8	

* The data are obtained from the lower side of the membrane (anodization end) after the removal of the barrier layer.

It was shown in [19] that, by using the SANS method, the degree of ordering of pores in the AA membranes strongly depends on the initial aluminum quality. Both chemical purity of the material and its crystalline structure affect this property.

However, it was stated in [20] that the influence of an aluminum substrate on the self-ordering of pores is limited only by the purity and crystallographic orientation of the Al substrate, while the density of dislocations, the size of grains, and their shape do not correlate with the degree of ordering of pores. This work is mainly aimed at studying the influence of the aluminum substrate microstructure (grain size) on the ordering of pores in the direction of their growth (in the longitudinal direction). Three series of AA membranes were studied which differed in the average distance between the pores and the thickness, and the average sizes of grains of the initial aluminum substrate differed inside each series. A linear dependence between the average grain size of an initial aluminum wafer and the average rectilinearity of pores for the synthesized membranes was revealed. It is assumed that the observed correlation is due to the influence of the crystallographic orientation of the grains of an initial aluminum wafer on the growth of a porous oxide film.

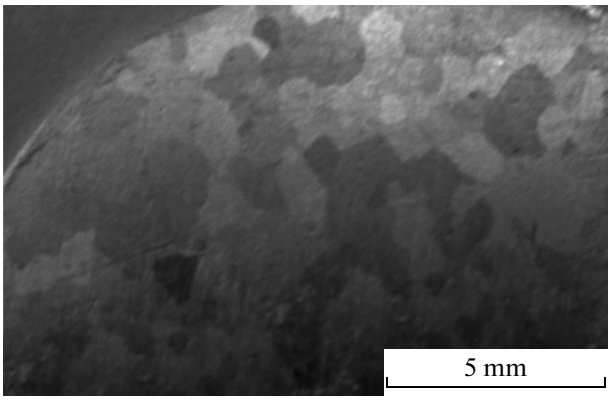

Fig. 1. Photograph of aluminum substrate prior to anodization.

SAMPLES UNDER STUDY AND EXPERIMENTAL SETUPS

Three series of samples of porous aluminum oxide with different distances between adjacent pores D_{int} were studied in our work. The series AAS ($D_{int} = 65$ nm) and AAO ($D_{int} = 105$ nm) were obtained by a two-stage anodic oxidation, while the samples HA ($D_{int} = 250–290$ nm) were synthesized under conditions of "hard" anodization [4]. The conditions of acquisition and the main structural parameters of the samples are presented in the table. As an initial material, we used wafers of high-purity polycrystalline Al (99.999%, a thickness of 0.5 mm, Goodfellow); their typical microstructure is presented in Fig. 1. Prior to anodization, aluminum was annealed at a temperature of 500°C in air for 12 h in order to remove mechanical stresses in metal and increase the sizes of grains. Then, the substrates were subjected to mechanical polishing with diamond pastes (Struers) up to a mirror luster and rinsed several times in acetone and deionized water in an ultrasound bath. The aluminum substrates differed

from each other in the average size of crystallites, which, according to the statistical processing of photographs for different substrates, varied from 0.1 to 0.9 mm^2. The area of oxide films was determined by the dimension of the window in the electrochemical cell and was constant (0.8 cm^2) for all samples studied. Inside a series, the samples were numbered according to an increase in the membrane thickness measured by scanning electron microscope (SEM) (the table). SEM images of AA membranes were obtained on a LEO Supra 50 VP device.

Experiments on the small-angle diffraction of neutrons were carried out on a SANS-2 (GKSS, Germany) setup with the use of neutrons with wavelengths of 6, 9, and 12 Å, monochromaticity of $\Delta\lambda/\lambda = 0.1$, and beam divergence of $\eta = 1.5$ mrad. The method of sample swinging was applied in the experiment [21]. The area of the sample region illuminated by the beam was 0.5 cm^2. The film was rotated with respect to a fixed vertical axis Y located in the film plane and normal to the direction of neutron-beam spreading by an angle of ±2.5° with a step of 0.1° (Fig. 2) [21]. The sample–detector distance amounted to 10 and 14 m, depending on the wavelength of neutrons used. Diffraction patterns were registered with the help of a position-sensitive detector with a resolution of 256 × 256 cells of 2.2 × 2.2 mm^2, each. The chosen geometry of the experiment made it possible to observe diffraction images in the range of transmitted pulses from 0.01 to 0.3 nm^{-1}.

Experiments on the small-angle diffraction of synchrotron radiation were carried out on a Dutch–Belgian line BM-26 DUBBLE [22, 23] of the European Synchrotron Radiation Facility (ESRF) in Grenoble (France). We used an X-ray beam with an energy of 13 keV (wavelength $\lambda = 0.95$ Å), transmission band of $\Delta\lambda/\lambda = 2 \times 10^{-4}$, and size of 0.5 × 0.5 mm^2 on the sample. In order to focus the beam onto a luminophor screen of a two-dimensional CCD detector (Photonic Science, 4008 × 2672 points of a size of 22 × 22 μm^2) located at a distance of 8 m from the sample, we used a set of berillium lenses. The samples were fixed on a goniometric head, which made it possible to orient them with respect to horizontal and vertical axes.

EXPERIMENTAL TECHNIQUE ON SMALL-ANGLE DIFFRACTION

The features of the small-angle diffraction of neutrons on the membranes of anodic aluminum oxide were studied in detail in [21]. It was shown that a well-correlated self-ordered hexagonal porous structure of AA films plays the role of an unusual two-dimensional diffraction grating for a neutron wave falling along the axis of pores. In this case, the thickness of the film (the length of pores) plays an important role in transferring from a weak to strong regime of interaction, which can

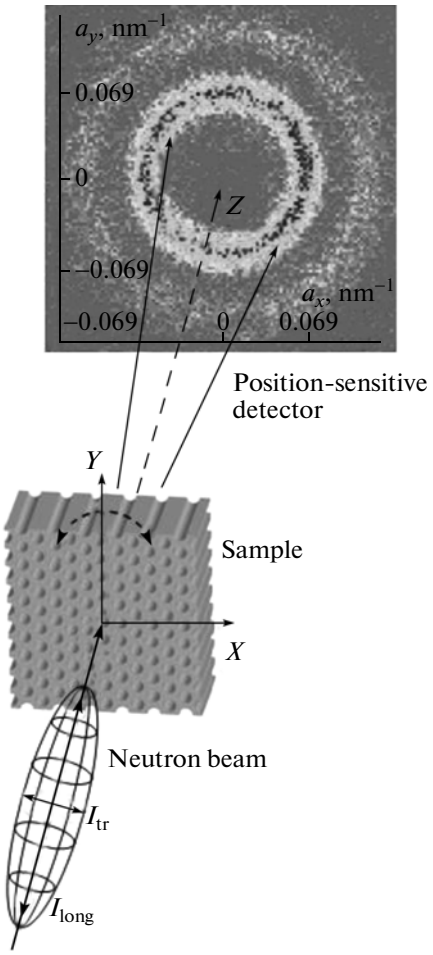

Fig. 2. Schematic image of an experiment on small-angle neutron scattering.

go out from the limits of the Born approximation. It is established that the long beam coherence along its spreading direction, typical for standard devices of small-angle scattering, is the reason for the high efficiency of neutron scattering at a porous structure of AA.

The concept of small-angle diffraction on a membrane with ordered pores developed in [21] describes diffraction as an interference of waves limited either by the degree of ordering of the structure under study or by the coherence of neutron beam (its resolution). The coherence of the neutron beam is determined as a region in the space in which an interference between the waves scattered inside a given sample volume is observed. The coherent volume is a wavepacket with the shape of an ellipsoid of revolution (Fig. 2). The coherent length of the neutron beam in the transverse direction ($l_{tr} = \lambda/\eta$) is determined mainly by an angle resolution of the beam η, i.e., by collimation. For the SANS-2 device, it amounts to $l_{tr} \approx 500$ nm; therefore, by scattering at a structure with a period of $D_{int} = 105$ nm, only $N = (l_{tr}/D_{int})^2 \approx 25$ pores from ~10^{10} illuminated

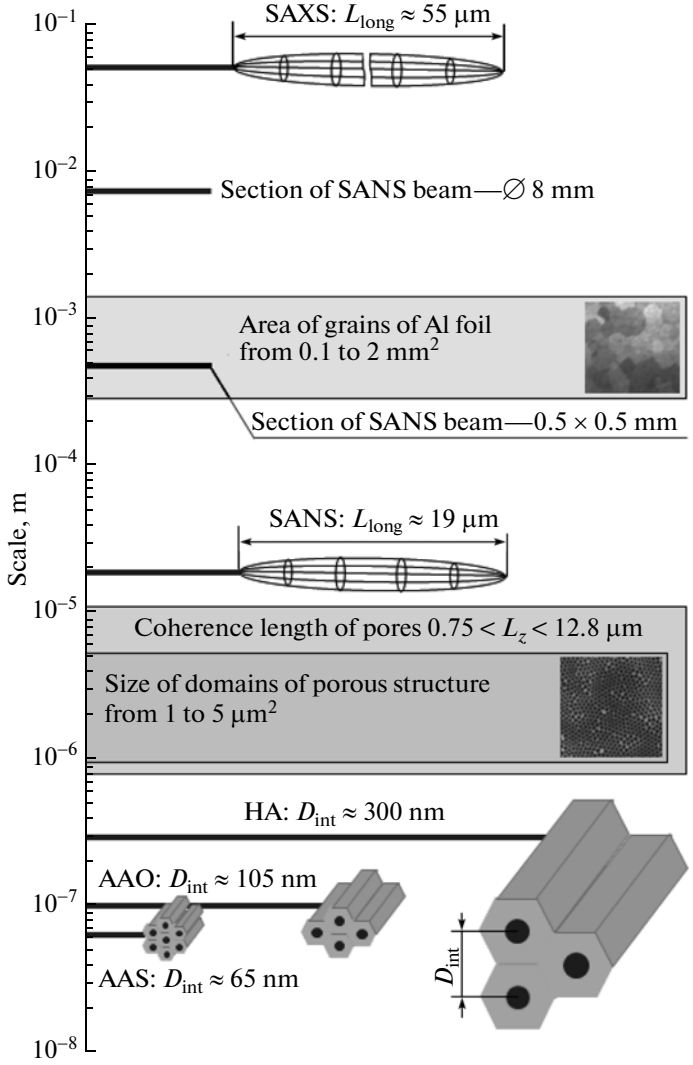

Fig. 3. Comparison of coherence lengths for neutron beams and X-ray radiation with typical sizes of the objects under study.

by the neutron beam appear to be inside of one coherent beam's volume. The pores located farther than l_{tr} are irradiated by waves with noncoherent phases.

The length of beam coherence in the longitudinal direction according to [21] can be estimated as

$$L_{long} \le \frac{l_{long}}{2\sin^2(\theta_B)} \sim \left(\frac{\lambda}{\Delta\lambda}\right)\frac{d^2}{\lambda}, \quad (1)$$

where $l_{long} = \lambda^2/\Delta\lambda$ is the length of coherence determined by the spectral width of the source $\Delta\lambda$. Here we used the Bragg law by replacing $\theta_B \to \lambda/2d$, where d is the interfacial distance. Thus, in a small-angle diffraction, the coherent length is inversely proportional to the wavelength of neutrons λ and in our case is limited by 50–100 μm. The longitudinal coherent length in the SANS experiment can be directly measured through the width of the Bragg peak, which is obtained as a function of the reflex intensity on the angle of sample swinging. The width of the swinging curve δ is connected with the coherent length L_z by the following expression:

$$L_{z,exp} = \frac{2\pi}{\Delta Q_z} = \frac{2\pi}{Q_{10}\sin\delta}. \quad (2)$$

If the longitudinal coherent length of the beam L_{long} exceeds the length of pores L, then in the case of their ideal ordering, $L_{z,exp}$, found in the experiment will be equal to the length of a pore L, i.e., the thickness of the sample. And, vice versa, if L_{long} is smaller than the length of ideal rectilinear pores or segments of pores L, then $L_{z,exp}$ will be equal to the coherent length of neutron beam L_{long}, which depends on λ (Eq. (1)). It was shown in [21] that, for the SANS-2 device, the parameter L_{long} for wavelengths $\lambda = 6$, 9, and 12 Å amounted to 19, 12.6, and 10 μm, respectively. For the device used for SAXS in our work (line BM-26 DUBBLE) the parameter L_{long} for the wavelength $\lambda = 0.95$ Å amounted to

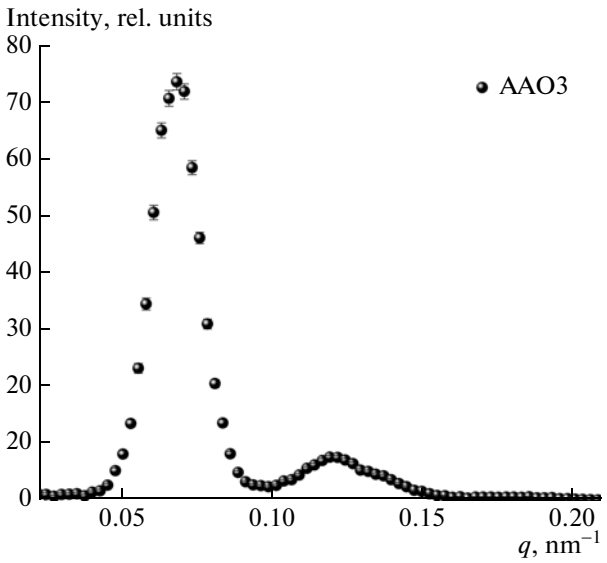

Fig. 4. Dependence of passed pulse of neutron scattering for the sample AAO3 at wavelength $\lambda = 0.6$ nm.

55 mm, while the transverse coherent length l_{tr} of the beam in the sample region was equal to 50 μm [24].

Figure 3 shows a comparison (in a logarithnic scale of linear dimensions) of main characteristics of the beams of neutrons and X-ray radiation with the structural parameters of the samples under study. It is clearly seen that the value of the longitudinal coherence L_{long} of the beams used allows us to measure the longitudinal coherent length of pores for all AA membranes studied.

RESULTS AND DISCUSSION

In SANS and SAXS experiments, for all samples studied independently of the thickness, concentric rings with the ratio of radii $1 : \sqrt{3} : 2$ were observed in the neutron and X-ray (synchrotron) diffraction patterns, which are a consequence of the presence of a great number of domains that are off-oriented with respect to each other (regions inside of which the pores form a strict two-dimensional hexagonal lattice) in a porous structure of anodic aluminum oxide [20]. By determining the position of the vector Q_{10} (Fig. 4) and taking into account the hexagonal structure of channel ordering, we found that the average distance between the pores D_{int} for the series of AAS and AAO samples amounted to 65 and 105 nm, respectively. This agrees well both with the microphotographs obtained from the upper (anodization start) and lower (anodization end) surfaces of membranes (Fig. 5a) and with the literature data [2]. Figure 6 shows the dependence of the average distance between the pores D_{int} on the thickness of membranes. We note that, for all samples of series AAS and AAO, the values of D_{int} practically do not change with the sample thickness;

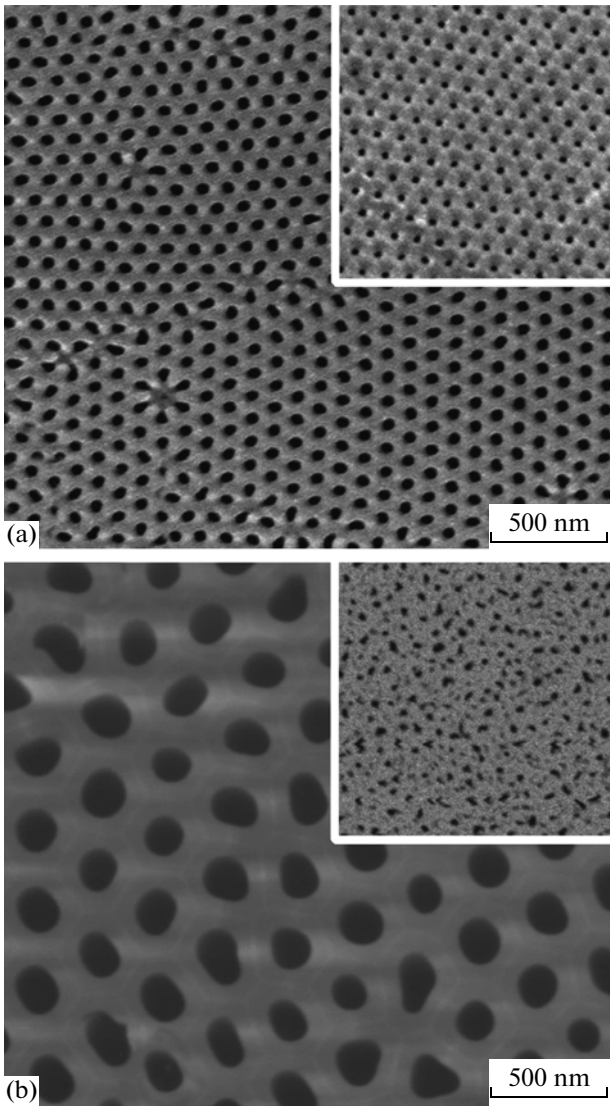

Fig. 5. SEM image of AA membranes from the side of the substrate after the selective dissolution of Al and removal of the barrier layer: (a) sample AAO4; (b) sample HA4. Inserts show photos of the upper part of the membrane formed at the beginning of the synthesis.

therefore, Fig. 6 shows only the results of SAXS measurements as an example.

On the contrary, in the case of obtaining oxide films by the method of hard anodization (series of samples HA), the average distance between the pores D_{int} gradually increases, with an increase in sample thickness L becoming constant only for samples with a thickness of more than 40 μm (Fig. 5b). Most clearly this is shown on the dependence obtained with the help of ESM. An increase in the distance between the pores D_{int} in the process of growth of the membranes of series HA is associated with the features of a hard anodization method [4]. At the initial stage, in order to prevent an electrical breakdown of the oxide film, the

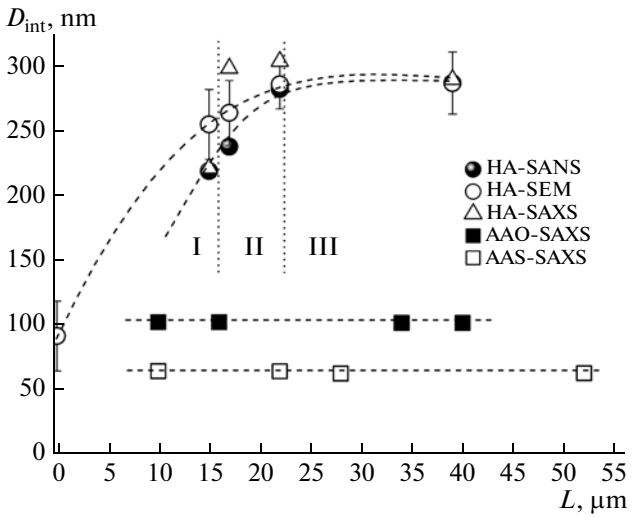

Fig. 6. Dependence of the average distance between the pores D_{int} on the thickness of samples according to the data of scanning electron microscope (SEM), small-angle neutron scattering (SANS) and small-angle X-ray scattering (SAXS).

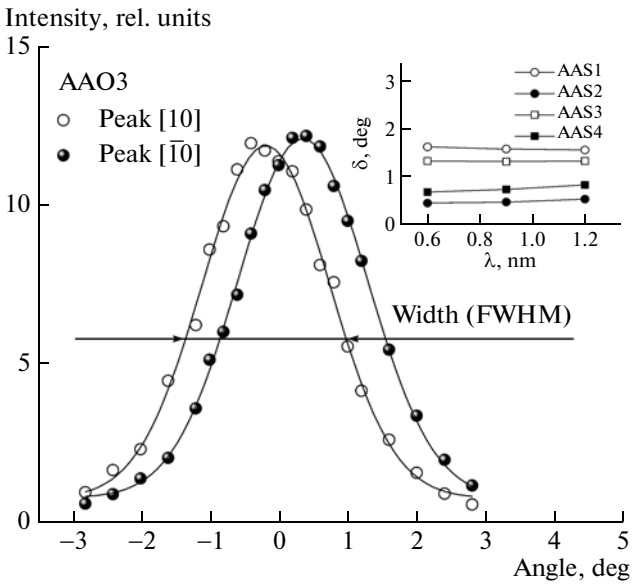

Fig. 7. Curves of swinging for reflexes [10] and [$\bar{1}$0] c of the sample AAO3 of 20 μm thickness. Small-angle diffraction patterns are obtained with the use of neutrons with a wavelength of λ = 9 Å. Solid line indicates the result of fitting the experimental curve by the Gaussian. The insert shows an example of the dependence of the width of the curve of swinging δ (FWHM) on the wavelength of neutrons for the samples of series AAS.

voltage is increased, gradually achieving a synthesis voltage of 140 V only after a certain time interval. It is worth noting that the distance between the pores depends linearly on the applied voltage. Thus, the average distance between the pores repeats the regime of changes in the voltage, i.e., increases at the initial stage and is constant under conditions of anodization at a fixed voltage. The structure of membranes obtained in the regime of hard anodization may be conditionally partitioned by the thickness into three zones (see Fig. 6).

The Ith zone is formed at the stage of the linear increase in the voltage to the required value (140 V) and is characterized by a quickly growing diameter and distance between the pores, which necessarily leads to the growth of some channels stopping [9]. A reconstruction of the porous structure strongly affects the rectilinearity of pores in the membrane. The existence of the IIth zone with a slowly increasing distance between the pores from the value achieved by the moment of the voltage reaching a constant value is due to a delay in the stabilization of all the system parameters (in particular, the temperature). Finally, the IIIth zone with a constant value of the distance between the pores characterizes the growth of the oxide film in a stable regime.

Figure 5b shows an image of the lower surface of the membrane HA4 after the removal of the barrier layer. The insert shows a microphotograph of the upper side, which visualizes the surface of the membrane formed at the beginning of the anodization process. It can be seen that the distance between the pores at the moment of their nucleation is much smaller than its average value D_{int}, typical for the lower side of the membrane. By comparing the curves obtained by SEM and SANS, we can see that, in the latter case, the calculated distance between the pores has a smaller value because the averaging takes place over the whole sample thickness.

In order to determine the longitudinal coherent length $L_{z,\,exp}$ in the structure of porous films of anodic aluminum oxide, the curves of swinging were obtained (Fig. 7). The experimental data were approximated by the Gauss function with the width δ, position $\alpha_{1,\,2}$, and an integral amplitude A_{int}.

The dependence of the width of the curve of swinging on the wavelength of neutrons for series AAS is shown in the insert to Fig. 7. The constancy of the width of the curve of swinging δ in dependence on λ indicates that the longitudinal coherent length $L_{z,\,exp}$ does not exceed the beam coherence in the corresponding direction L_{long} = 19, 12.6, and 10 μm for wavelengths 6, 9, and 12 Å, respectively [21].

The values of $L_{z,\,exp}$ calculated from the data of SANS and SAXS vary from 0.75 to 13 μm (see Fig. 8). We note that in all cases the longitudinal correlation length of channels (the distance at which the pores decline from their axis by a value not exceeding D_{int}) appears to be smaller than the membrane thickness. A distortion of pores along the direction of their growth may be associated both with the reconstruction of the porous structure in the process of self-organization [25] and may be a consequence of the fine-grained structure of anodized aluminum substrates (Fig. 1).

In order to check these hypotheses, we built plots of the dependences of the coherent length $L_{z,\,exp}$ on the

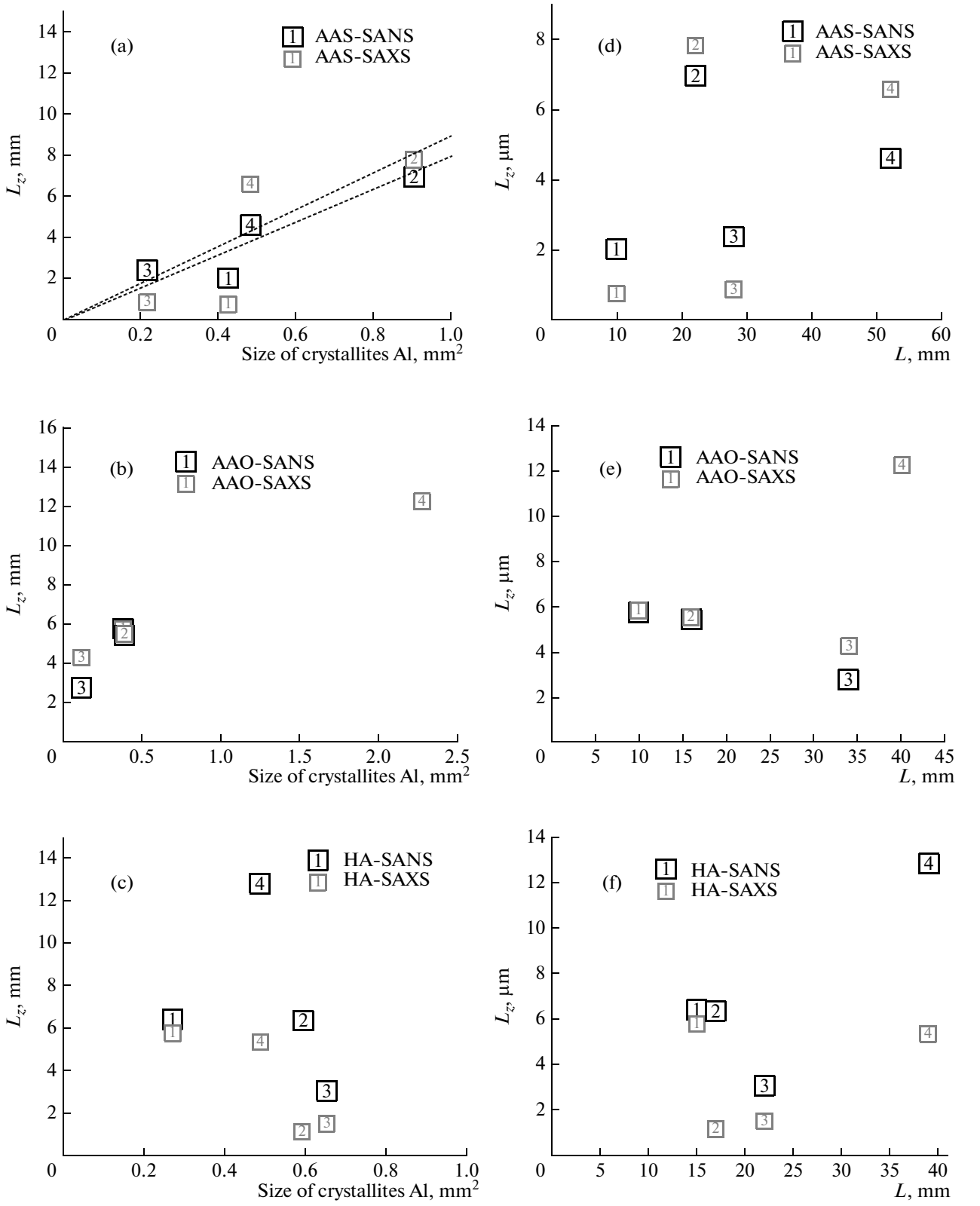

Fig. 8. Dependences of coherent length L_z on the average dimension of crystallites of aluminum substrate (a–c) and on the thickness of membranes L (d–f). The data are given for three series of samples: (a, d) AAS, (b, e) AAO, and (c, f) HA. The coherent length L_z was calculated in the process of data processing of SANS and SAXS. The number of the point in the plot corresponds to the number of the sample inside the series.

average size of grains of the aluminum substrate of the corresponding sample (Figs. 8a–8c), as well as on the sample thickness L (Figs. 8d–8f). It can be seen that, in the case of the samples synthesized at a constant voltage (series AAS and AAO), the value of L_z characterizing the average length of the rectilinear segments of pores substantially increases with the growth in the average grain size of an Al substrate (Figs. 8a, 8b). The duration of anodization, which determines the thickness of a porous film, plays a secondary role: L_z for samples obtained in the same conditions on substrates with a similar microstructure (see, e.g., AAS1 and AAS4 in Fig. 8a) appears to be longer for a thicker oxide film.

It should be noted that a difference in the values of the coherent lengths L_z obtained by SANS and SAXS methods is associated with the area of an illuminated sample region. In the case of the SANS method, practically the whole surface of an oxide membrane is irradiated, while in the case of SAXS method a region of one or several crystallites of the substrate is irradiated (see Fig. 3). We note that the longitudinal coherent length of pores both within the whole sample and in a region of one crystallite remains a value of the same order of magnitude. This is associated with the predominant growth of channels in the direction normal to the substrate surface defined by the lines of force of the electric field.

For samples of series HA, an explicit correlation between the longitudinal coherence of pores and the average grain size was not observed, which is due to the simultaneous influence of both the crystalline structure of the substrate and a change in the average distance between the pores at the initial stage of synthesis by an increase in the anodizing voltage. We note that a maximum value of L_z in the given series was observed for the thickest sample HA4. This is not surprising because the direct channels are formed only at the final stage, when all parameters of anodization (voltage and temperature) are constant.

CONCLUSIONS

Using complementary methods of the small-angle diffraction of neutron and synchrotron radiations, as well as SEM, the value of the longitudinal coherence of the system of pores for the films of anodic aluminum oxide obtained in various conditions is quantitatively determined and the dependence between the rectilinearity of channels and grain size of the initial aluminum substrate is established. It is shown experimentally that, in the films of anodic aluminum oxide obtained by the method of two-stage oxidation of coarse-crystalline aluminum in the regime resulting in the formation of a self-organized structure, the longitudinal correlation length of the system of pores can exceed 10 μm.

The growth of the longitudinal coherence of the structure with an increase in the average size of metal grains can be accounted for by the influence of the crystallographic orientation of individual crystallites on the growth of oxide film [25, 26] due to different rates of oxidation of different crystal faces. This suggestion will be a subject for further studies.

ACKNOWLEDGMENTS

The Russian authors thank the Russian Foundation for Basic Research (grant no. 10-02-00634) and the Ministry of Education and Science of Russian Federation (grant no. 16.513.11.3011) for support and Research Centers HZG (Germany) and ESRF (France) for hospitality.

REFERENCES

1. S. Shingubara, J. Nanopart. Res. **5**, 17 (2003).
2. K. Nielsch, J. Choi, K. Schwirn, et al., Nano Lett. **2**, 677 (2002).
3. J. P. O'Sullivan and G. C. Wood, Proc. R. Soc. London Ser. **317**, 511 (1970).
4. W. Lee, R. Ji, U. Gosele, et al., Nat. Mater **5**, 741 (2006).
5. S. Shingubara, O. Okino, Y. Sayama, et al., Jpn. J. Appl. Phys. **36**, 7791 (1997).
6. Y. B. Li, M. J. Zheng, and L. Ma, Appl. Phys. Lett. **91**, 073109 (2007).
7. P. C. Stair, C. Marshall, G. Xiong, et al., Top. Catal. **39**, 213 (2006).
8. D. I. Petukhov, A. A. Eliseev, D. A. Buldakov, et al., Membrany. Ser. Kritich. Tekhn. **43**, 16 (2009).
9. D. I. Petukhov, K. S. Napolskii, and A. A. Eliseev, Nanotecnology **23**, 335601 (2012).
10. Y. Zhang, G. Li, Y. Wu, et al., Adv. Mater. **14**, 1227 (2002).
11. K. S. Napolskii, P. J. Barczuk, S. Yu. Vassiliev, et al., Electrochim. Acta **52**, 7910 (2007).
12. M. R. Lukatskaya, L. A. Trusov, A. A. Eliseev, et al., Chem. Commun. **47**, 2396 (2011).
13. I. V. Roslyakov, K. S. Napol'skii, A. A. Eliseev, et al., Nanotech. Russ. **4** (3–4), 176 (2009).
14. K. S. Napolskii, A. P. Chumakov, S. V. Grigoriev, et al., Phys. B **404**, 2568 (2009).
15. H. Masuda, M. Tamada, F. Matsumoto, et al., Adv. Mater. **18**, 213 (2006).
16. P. Banerjee, I. Perez, L. Henn-Lecordier, et al., Nature Nanotech. **4**, 292 (2009).
17. K. Nielsch, R. B. Wehrspohn, J. Barthel, et al., Appl. Phys. Lett. **79**, 1360 (2001).
18. P. Mardilovich, D. Routkevitch, and A. Govyadinov, Electrochem. Soc. Proc. **200-19**, 33–42 (2000).
19. S. V. Grigor'ev, N. A. Grigor'eva, A. V. Syromyatnikov, et al., JETP Lett. **85** (12), 605 (2007).
20. G. Beck and K. Petrikowski, Surf. Coat. Technol. **202**, 5084 (2008).
21. S. V. Grigoriev, A. V. Syromyatnikov, A. P. Chumakov, et al., Phys. Rev. B **81**, 125405 (2010).
22. M. Borsboom, W. Bras, I. Cerjak, et al., J. Synchrotron Rad. **5**, 518 (1998).
23. A. V. Petukhov, J. H. J. Thijssen, D. C.'t Hart, et al., J. Appl. Crystallogr. **39**, 137 (2006).
24. K. S. Napolskii, I. V. Roslyakov, A. A. Eliseev, et al., J. Appl. Crystallogr. **43**, 531 (2010).
25. K. S. Napolskii, I. V. Roslyakov, A. A. Eliseev, et al., J. Phys. Chem. C **115**, 23726 (2011).
26. K. S. Napolskii, I. V. Roslyakov, A. Y. Romanchuk, et al., J. Mater. Chem. **22**, 11922 (2012).

Translated by R. Litvinov